PROCEEDINGS OF ECOS 2023 - THE 36TH INTERNATIONAL CONFERENCE ON
EFFICIENCY, COST, OPTIMIZATION, SIMULATION AND ENVIRONMENTAL IMPACT OF ENERGY SYSTEMS
25-30 JUNE, 2023, LAS PALMAS DE GRAN CANARIA, SPAIN

Low-temperature compressed air energy storage with reversibly operable turbo- and piston machines

Markus Hadam[a], Marcus Budt[b]

[a] Fraunhofer UMSICHT, Oberhausen, Germany, markus.hadam@umsicht.fraunhofer.de
[b] Fraunhofer UMSICHT, Oberhausen, Germany, marcus.budt@umsicht.fraunhofer.de

Abstract:

Adiabatic compressed air energy storage (A-CAES) is a promising storage technology to face the challenges of high shares of renewable energies in an energy system by storing electric energy for periods of several hours up to weeks. In order to reduce the investment costs and increase the flexibility of the storage system, the so called KompEx LTA-CAES® was developed by Fraunhofer UMSICHT. This new A-CAES concept is using a combination of reversibly operable turbo- and piston machines (KompEx machines). Doing so, these modules can achieve wide CAS pressure ranges (corresponding to high exergy densities) and thus can be combined with any compressed air storage volume. To realize efficient and stable operation despite a wide pressure range, a suitable control strategy of both KompEx machines is required. This paper investigates the introduced A-CAES system by a dynamic simulation, focusing on the interaction and synergy between the reversibly operable turbo- and piston machines. Results indicate that the roundtrip efficiency of this system is expected to be at the low end (55,5%) of literature values for A-CAES (52–66% for low-temperature A-CAES), which is relatively high compared to published A-CAES systems considering similar pressure ranges.

Keywords:

Compressed Air Energy Storage; Thermodynamics; Energy Storage; Dynamic Simulation

1. Introduction

A-CAES systems have the potential to play an important role in realizing a sustainable energy supply infrastructure based on renewable energy. The general interest in A-CAES is illustrated by many R&D activities all over the world in recent years. Nevertheless, the economically viable implementation of A-CAES plants is a great challenge under political and economic conditions in most countries at the present time – and probably also in near future.

This paper gives an overview of published thermodynamically investigated A-CAES concepts. Furthermore, a new low-temperature A-CAES concept developed by Fraunhofer UMSICHT called »KompEx LTA-CAES® modular« is presented (Section 3), which aims to overcome current barriers regarding the economic realization of A-CAES. Special features are the modular design and the use of reversibly operable turbo- and piston machines (KompEx machines).

2. State of the art

Although the individual components of many A-CAES concepts are commercially available, A-CAES systems are still almost exclusively in the R&D phase due to economic barriers. For this purpose, several demonstration plants have been built worldwide [1–4]. The first commercial adiabatic CAES plant was commissioned in Goderich (Ontario, USA) in 2019 [5], and others are currently under construction in China [6]. Nevertheless, A-CAES are still mainly studied on a theoretical level, which is illustrated by a large number of thermodynamic studies published in the last decades. This section briefly introduces the general function and typical classification of A-CAES systems and gives an overview of published layouts.

2.1. Functional principle of adiabatic CAES

The basic principle and the main components of adiabatic CAES are shown in Figure 1. During the charging process, ambient air is compressed by electrically driven compressors (C). The heated compressed air is cooled and stored in a compressed air storage volume (CAS), while the thermal energy is temporarily stored in a separate thermal energy storage (TES). During discharging, the stored compressed air is released from the CAS, heated via the TES and expanded in expanders (E) to generate electricity via generators.

https://doi.org/10.52202/069564-0190

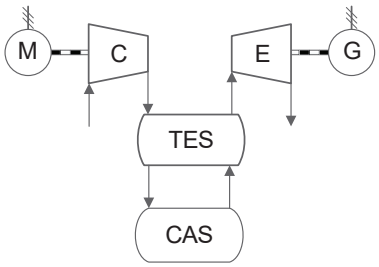

Figure 1. General block diagram of A-CAES (based on [7]).

The plant layout design, suitable technologies and the resulting operating behaviour of A-CAES systems are crucially dependent on the addressed storage temperature. Therefore, the following section gives an overview of general plant layouts and their special characteristics.

2.2. Classification of A-CAES

According to the importance of the process temperature, A-CAES can be divided into three different process types [8]:

- High temperature processes (HT) with temperatures above 400 °C
- Medium-temperature processes (MT) with temperatures between 200 °C and 400 °C
- Low-temperature processes (LT) with temperatures below 200 °C

The process temperature is essentially determined by the number of the used compression stages and heat management. In HT processes, ambient air is compressed via one or two stages, which leads to high process temperatures at corresponding final pressures. In LT processes, multi-staged compressors with intercooling are used, resulting in lower process temperatures. Higher process temperatures are leading to generally higher cycle efficiencies (Figure 2) but also to higher investment costs, since special thermally resilient components are required. Furthermore, the start-up times are limited to 10–15 minutes due to the high thermal stresses in the components [48]. A-CAES systems with lower process temperatures, in contrast, are technically easier to design (e. g. a simple storage medium such as water can be used), resulting in lower investment costs. Furthermore, lower thermal stresses are allowing faster start-up times (down to < 5 min.) and thus the participation in certain electricity markets like the ancillary service.
In contrast to a Carnot cycle process, the maximum process temperature has only a minor influence on the cycle efficiency of A-CAES systems (Figure *2*). The illustrated efficiency range (solid lines) is based on a simple equation introduced by Kreid [9], where fixed design values for relevant main components like efficiency of motor and generator, compressor and expander as well as pressure and thermal losses are taken into account. The efficiency range illustrated in Figure *2* is resulting by assuming a turbomachine efficiency between 70 and 85 %. The plotted data points are representing electrical cycle efficiencies of adiabatic plant layouts calculated in thermodynamical studies (Table A.1). The decreasing efficiency for lower storage temperatures is resulting from proportionally higher thermal losses at constant temperature gradients [10].

2.3. Key parameters of published A-CAES concepts

Published A-CAES concepts are varying widely regarding the design of compression/expansion stages, thermal storage and compressed air storage as well as implemented control strategies. To highlight the special features of the developed KompEx LTA-CAES®, the following section briefly provides an overview of typical plant layouts and key performance indicators of published A-CAES concepts.

Storage temperature and used thermal storage media

The storage temperature of the thermal energy storage of A-CAES plants is dependent on the final CAS pressure as well as on the design and heat management of the compression train. Depending on the process type, water, thermal oils or rockfills are most commonly used as thermal storage media (Table A.1).

Cycle efficiency

The plant efficiencies calculated in published A-CAES studies are showing a logarithmic dependency on the storage temperature (trend line in Figure *2*) and mostly a reasonable agreement with the predicted efficiency range according to Kreid [9]. The two upper outliers ([11, 12]) can be explained by the comparatively high design efficiencies of the compression and expansion machines of 88 to 92 % assumed in each of these papers. In comparison, the calculation of the upper cycle efficiency according to Kreid [9] is based on a maximum efficiency assumption of 85 %.

Several thermodynamic studies [13–19] are calculating A-CAES cycle efficiencies which are – in some cases significantly – below the cycle efficiency range according to Kreid [9] (Figure *2*). A closer look at the

https://doi.org/10.52202/069564-0190

corresponding plant layouts shows that in these the CAS volumes are operated within a relatively wide pressure range (Table A.1). As a result, the compressors are increasingly operated outside their optimum. Furthermore, the corresponding plant layouts are using throttle valves to ensure a constant inlet pressure in the expansion machines during the discharging process. This measure is leading to an optimum operation of the expanders at the cost of high losses of the usable potential energy stored in the CAS. These losses are rising with larger operating pressure differences of the CAS. The two negative effects described are leading to relatively low cycle efficiencies.

The developed KompEx LTA-CAES® addresses a relatively wide CAS pressure range but nevertheless reaches a comparatively higher electrical efficiency of 55.53 % (point 14 in Figure 2). This is obtained by the special constellation of the compressors/expanders and the implemented control strategy of the plant layout, which will be discussed later.

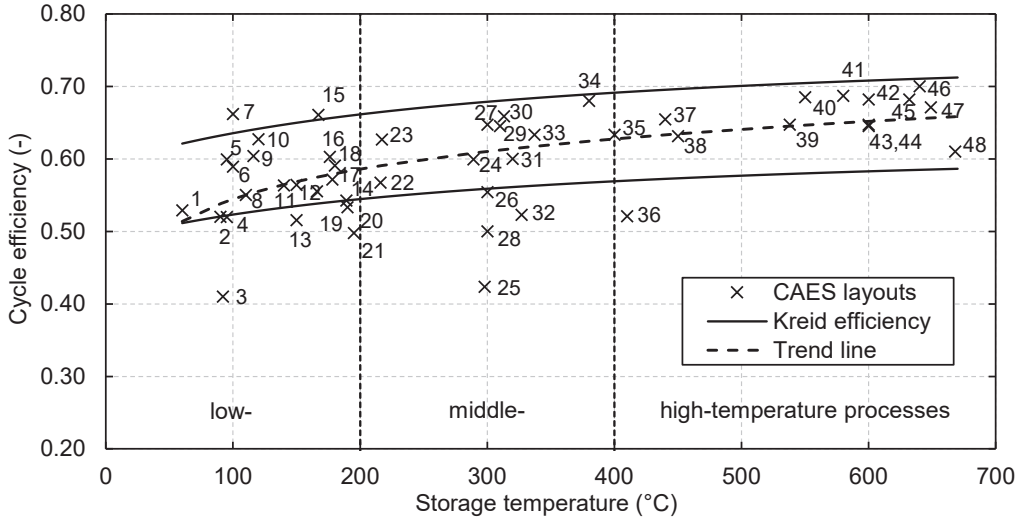

Figure 2. Predicted CAES cycle efficiencies according to [9] and calculated by published A-CAES studies depending on storage temperature (based on [8]); see Table A.1 for the literature allocation of the CAES layout data points.

Charging and discharging power

The designed installed charging/discharging capacity of investigated system layouts usually is depending on the addressed application. The focus of past studies is mostly on huge central applications. This usually includes storage systems that are used for the temporal shifting of large amounts of energy with high electrical power (> 20 MW_{el}, Table A.1). These systems usually operate at the medium and high-voltage level and can provide grid services such as minute reserves. In contrast, decentralized storage concepts are characterized by lower charging/discharging powers and energy storage volumes. They are usually located near the consumer and are suitable to compensate generation and consumption peaks or to backup island grids. Both centralized and decentralized storage applications are considered promising, especially when coupled with fluctuating renewable energies like wind turbines or photovoltaic plants. [20, 21]

CAS technology and exergy density

The amount of energy to be stored as well as geographical conditions have a decisive influence on the choice of a suitable CAS technology. In studies on centralized A-CAES concepts, underground salt caverns are generally used to store the compressed air (Table A.1), since they have low specific investment costs (€/m³) when storing large amounts of energy. The maximum pressure and the realizable pressure difference of salt caverns are strongly dependent on their geological characteristics. In corresponding studies, the salt caverns are commonly operated with pressure differences of less than 40 bar.

In the field of decentralized applications, storage capacities below 20 MW_{el} are usually required. Due to the strong geographical dependency and the high specific investment costs of salt caverns when storing smaller energy quantities, they are unsuitable in this case. Therefore, artificial CAS technologies with smaller storage volumes, e. g. in the form of steel tubes, steel cylinders or steel spheres are more appropriate in decentralized applications (Table A.1) [20]. In contrast to underground salt caverns, the maximum storage pressure and the realizable operating pressure difference for these CAS systems are much higher. Thus, significantly higher exergy densities can be achieved, which is of great importance for the economic operation of artificial CAS technologies as they have relatively high specific investment costs.

https://doi.org/10.52202/069564-0190

As an example: When charging the CAS isothermally at 15 °C, a pressure range of 80–100 bar results in an exergy density of about 2.5 kWh/m³, while a pressure range of 60–100 bar results in about 5 kWh/m³ [23].

3. KompEx LTA-CAES®

This section describes the new A-CAES concept which has been developed within the joint project »KompEx LTA-CAES® modular - Development of a modular low-temperature compressed air energy storage system with reversibly operable machines (KompEx)« funded by the German Federal Ministry for Economic Affairs and Climate Action [22]. The goal was to overcome existing barriers regarding the economic realization of adiabatic CAES based on four novel approaches. (1) A modular design to reduce unit costs through possible serial production. (2) Low storage temperatures to enable short start-up times and thus participation in profitable electricity markets. (3) To reduce investment costs, reversibly operable machine sets (KompEx machines) for compressed air are being developed. (4) By combining turbo- and piston machines, wide pressure ranges within the CAS can be realized, enabling an economical use of various CAS technologies, and thus reducing the geographical dependency from salt caverns.

3.1. Plant Layout

Figure 3 is showing the simplified block diagram of a KompEx module. Ambient air is compressed to a certain intermediate pressure via an intercooled multistage radial turbomachine ($TM_{1\text{-}n}$) driven by a motor-generator (MG). The Intercooling is carried out via plate heat exchangers ($HX_{1\text{-}n}$). The occurring thermal energy is stored by a two-tank liquid thermal energy storage – referred as low-pressure thermal energy storage ($LP\text{-}TES_{hot/cold}$) in the following. Depending on the current operating state (charging/discharging), the heat storage medium (water) is transported between the two tanks via a pump through the heat exchangers. The process section consisting of motor generator, radial turbomachine, heat exchanger and LP-TES is referred as low-pressure process (LP-process) in the following.

After the LP-process, high-pressure piston machines ($PM_{1\text{-}n}$) – each consisting of 2 individually operable cylinders – are compressing the low-pressure air to the pressure level of the CAS, which varies with the filling level. Each of the piston machines has its own motor-generator to switch single machines on and off during the charging or discharging process, which is important for the implemented process control strategy (Section 3.3). Due to the higher pressure ratios and thus higher outlet temperatures of the piston machines, the respective occurring thermal energy is stored via a high-pressure thermal energy storage (HP-TES) in the form of an indirect-flow concrete storage. Using two separated TES systems is resulting to a higher exergetic efficiency of the overall process. A trim cooler (TC) connected downstream of the HP-TES is ensuring low inlet temperatures to the CAS in order to reduce the required storage volume. The section consisting of piston machines including the motor-generators, HP-TES and trim cooler corresponds to the high-pressure process (HP-process) of the KompEx LTA-CAES®.

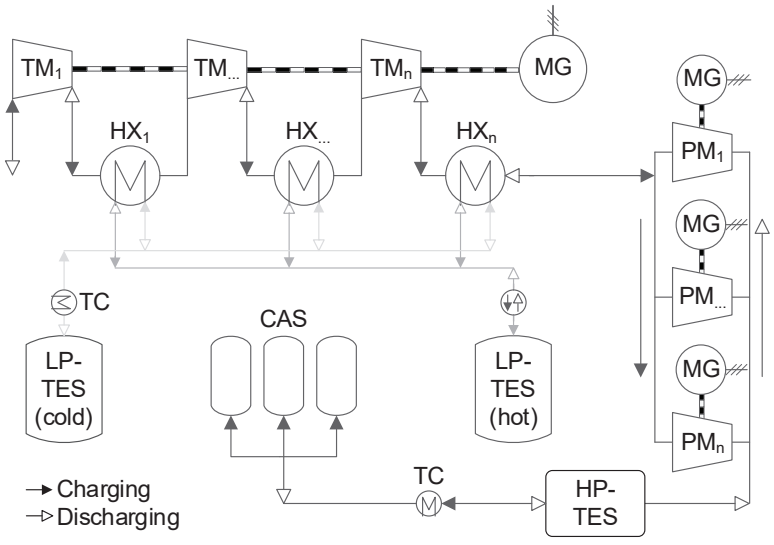

Figure 3. Simplified block diagram of the KompEx LTA-CAES® module [23].

During the discharging process, the compressed air is flowing through the same components in the reverse direction. The compressed air is heated via the respective TES system and then expanded in the KompEx machines to generate electricity in the motor-generators. By using the reversibly operable KompEx machines, a complete machinery train including expanders, heat exchangers and pipes can be omitted resulting in

https://doi.org/10.52202/069564-0190

reduced investment costs. Furthermore, the synergetic use of turbo- and piston machines enables an efficient operation of wide pressure ranges and thus the option of using artificial CAS technologies in addition to salt caverns. Finally, the described KompEx layout represents one module. In order to achieve higher storage capacities, several modules can be interconnected. This provides greater flexibility in terms of suitable storage applications and the potential to reduce costs by series production.

3.2. Design parameters

The design parameters of the investigated KompEx LTA-CAES® module were developed within the KompEx project (Table 1). The use of reversibly operable turbo- and piston machines in A-CAES systems leads to some special design constraints compared to concepts with separate compressors and expanders. Since the compression and expansion of the compressed air in the KompEx system are performed by the same machines, the respective design volume flows and thus the charging and discharging power are linked. This also applies to the design efficiency of the compression and expansion mode of the KompEx machines. Optimizing the KompEx machines for one of the two operating modes has a direct influence on the efficiency of the other one. Consequently, a compromise design of the KompEx machines is required. As a result, lower nominal efficiencies can be expected compared to separated state-of-the-art turbo- and piston machines. The listed nominal efficiencies (Table 1) of both machine types for each operation mode were calculated by detailed CFD simulations within the KompEx project [22]. Furthermore, the KompEx layout is specially designed for decentralized storage applications. Therefore, the CAS volume is operated within a wide pressure range to achieve high exergy densities and thus to reduce the investment costs of the CAS volume.

Table 1. Design parameters of the investigated KompEx LTA-CAES® module [23].

Design parameter	Value	Unit
Nominal electrical Power of charging	2	MW_{el}
Nominal electrical Power of discharging	1	MW_{el}
Pol. nominal efficiency in compression mode of TM	82	%
Is. nominal efficiency in expansion mode of TM	85	%
Pol. nominal efficiency in compression mode of PM	76	%
Is. nominal efficiency in expansion mode of PM	80	%
CAS volume	1.304	m^3
CAS pressure range	40–100	bar
Number of turbomachines	3	-
Number of piston machines	11	-

3.3. Control strategy

There are many different possible applications for energy storages. Examples include trading on spot markets, providing ancillary services, increasing power generation from fluctuating renewable energies and supplying electricity in off-grid regions. In some cases, a combination of different applications is also possible. Depending on the storage application, different regulatory and technical requirements must be fulfilled by the storage system. In particular, participation in ancillary services is associated with strong restrictions. The frequency restoration reserve relevant for CAES systems, for example, is requiring a constant power input and output over a defined period with a maximum deviation of 5 % [24, 25].

The KompEx LTA-CAES® is designed to cover a wide range of the mentioned applications. Therefore, a control strategy was implemented to provide constant charging and discharging power, which is necessary due to the strongly varying storage pressure. For this purpose, the turbomachine stages are designed with variable diffusor guide vanes, which enables a wide operating range of the entire turbomachinery train. In addition, single cylinders of the piston machines can be switched on and off during operation to adjust the pressure between turbo- and piston machines (Section 4.1). Furthermore, the valve on the pressure side of the piston machines can be adjusted during discharging process, which enables a less fluctuating controlling in contrast to the charging process.

3.4. Dynamic model

The investigation of the KompEx LTA-CAES® is carried out with a dynamic plant model developed in Modelica/Dymola considering real property data of humid air. The operation behaviour of the KompEx machines is modelled via black box models with implemented polynomial surface functions. In these, the efficiencies and pressure ratios of each compressor/expander stage are determined as a function of the volume flow and the respective actuating value (guide vane angle in the turbomachines; valve position in the piston machines). To consider thermal losses to the environment, the heat exchanger, ND-TES, HD-TES, CAS and piston machines are modelled diabatically. The dynamic behaviour of the heat exchangers and the HD-TES are considered by two-dimensional discretized models (finite volume method). Detailed information

regarding the dynamic model, the implemented KompEx surface functions and equations of each component can be found in [23]. The operating schedule of the simulated A-CAES is predefined via a time series in the form of the electrical charging and discharging power. The actual plant power is compared with the predefined power by means of a PID controller and adjusted accordingly via the control variables implemented in the turbo and piston machines.

4. Results and discussion

The introduced KompEx plant layout was investigated in detail regarding dynamic interactions, partial load and cycling behaviour as well as occurring exergetic losses. In this paper, the focus is only on the control strategy and interaction between the turbo- and piston machines. More detailed investigations can be found in [23].

4.1. Reference storage cycle

The dynamic curves of relevant process parameters presented in the following are based on the dynamic system simulation of a full storage cycle at nominal load operation and steady state. The system is considered to be steady state when the stored exergy in the CAS and TES after a full cycle is equal to that of the previous cycle within a deviation of ±1.0 %.

The charging and discharging process is taking about eight hours, the storage process is set up to four hours. During charging process the storage pressure in the CAS rises continuously to the maximum pressure of 100 bar, drops slightly during storage process due to thermal losses to the environment and decreases to the minimum storage pressure of 40 bar during discharging (Figure 4, diagram top left). The electrical power consumption and generation is kept practically constant (diagram top right) during the charging and discharging process via the mass flow rate (diagram bottom left), which is adjusted by the implemented control systems (diagram top right). This is necessary since the total pressure ratio and thus power of the turbo- and piston machines varies at constant mass flow rate. The exergetic charging and discharging efficiency is strongly dependent on the current operating point resp. storage pressure (diagram bottom right). This illustrates that a dynamic process simulation is crucial for a realistic representation and evaluation of the overall system. The characteristic behaviour of the illustrated process variables is primarily resulting from the interaction of the turbo- and piston machines and the implemented system control, which are described in detail in the following section.

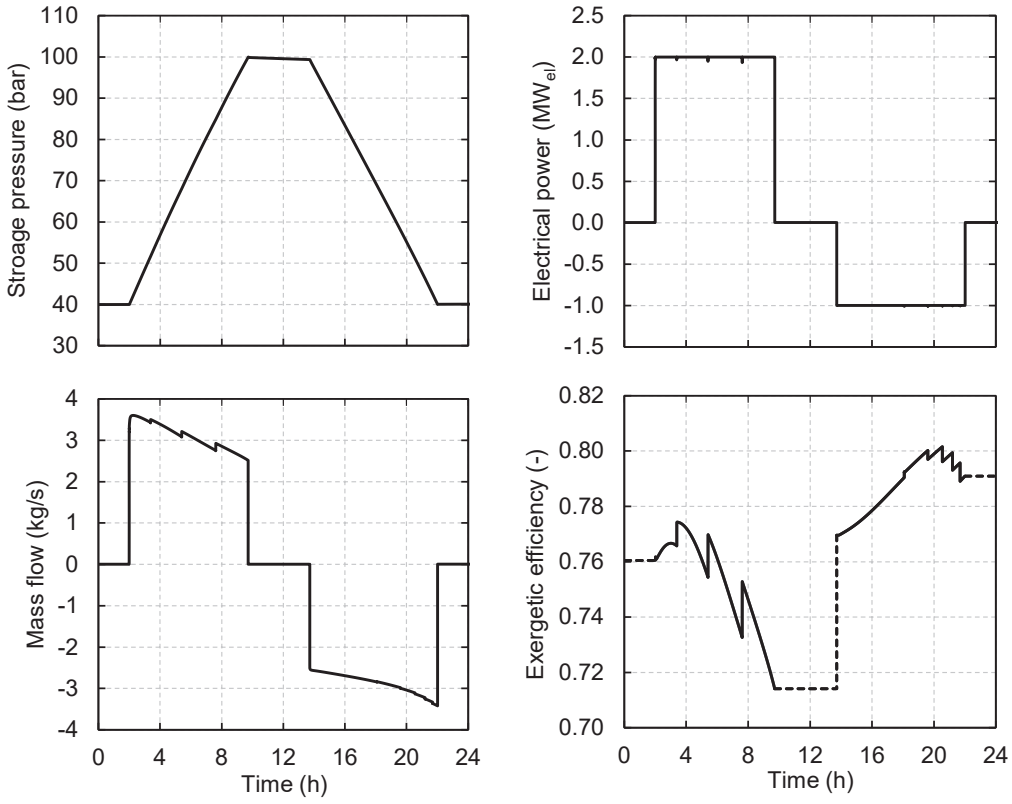

Figure 4. Storage pressure, electrical charging and discharging power, mass flow and charging and discharging efficiency of the reference storage cycle [23].

https://doi.org/10.52202/069564-0190

4.2. Interaction of the turbo- and piston machines

This section describes the control strategy and interaction of the turbo- and piston machines during a full charging process. The dynamic process behaviour of adiabatic CAES is essentially determined by the transient behaviour of the CAS. Therefore, the process parameters regarding the charging process are plotted as a function of the storage pressure (Figure 5). The pressure ratio (increasing from 3.58 to 8.88) and thus electrical power consumption of the piston machines is rising from 0.81 to 1.12 MW_{el} (diagram top left) due to the increasing storage pressure. This power increase is compensated by adjusting the mass flow via the variable guide vanes of the turbomachines reducing its power consumption (diagram top right).

The varying mass flow caused by the control system is resulting in a continuously varying operating point of the turbo- and piston machines, which is illustrated by the intermediate pressure (pressure between turbo- and piston machines) fluctuating during the charging process (Figure 5, diagram bottom left). The peaks observed in the shown diagrams are caused by the shutdown of single piston cylinders during the charging process, which is controlled by a discrete control loop. The reduction of the mass flow to provide a constant overall power consumption leads to an increased pressure ratio of the piston machines according to its implemented characteristic surface function. As a result, the pressure ratio of the three-stage turbomachine and thus the intermediate pressure decreases continuously. In order to ensure both machine types are operating efficiently and within their operation range, a piston cylinder is switched off at a specified minimum intermediate pressure of 11 bar (diagram bottom right). This causes an abrupt drop in the mass flow and thus in the electrical power consumption of the piston machinery train. The control system integrated in the turbomachinery train compensates this power drop by adjusting the guide vane angles of each stage resulting in an increased mass flow and power consumption. Due to the described abrupt interactions, both machine types are reaching a new operation point with a raised intermediate pressure. Further charging of the KompEx LTA-CAES® again causes the intermediate pressure to decrease until the next piston cylinder is switched off.

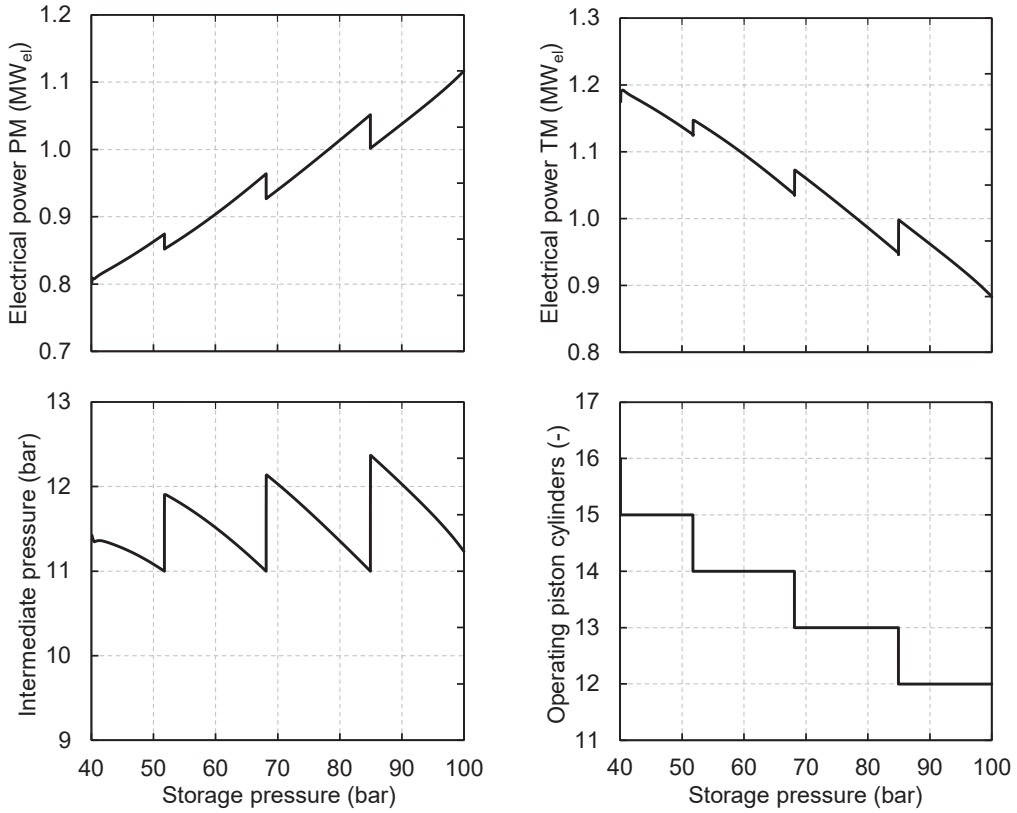

Figure 5. Electrical power of turbo- and piston machines, intermediate pressure and number of operating piston cylinders as function of the storage pressure for the reference storage cycle [23].

https://doi.org/10.52202/069564-0190

4.3. Part load behaviour

An important aspect that is often neglected in the literature investigating on A-CAES concepts using isochoric CAS is the influence of the varying CAS pressure range on the part load ability when a constant charging and discharging power shall be provided. To illustrate the described relationship, Figure 6 is showing a complete charging process (40 to 100 bar) with minimum and maximum power consumption of the KompEx system drawn in the efficiency map of the three-stage turbomachinery. Its operation limits are the limiting factor for the minimal operable power load of the overall system. The normalized efficiency and volume flow rate of 1.0 correspond to the respective design values.

During the charging process and thus rising storage pressure, the volume flow rate is reduced by the control system to realize a constant electrical power consumption of the overall system (Figure 4). Therefore, the volume flow rate must be reduced by up to 30 % via the outlet guide vanes of the turbomachine stages when charging with maximal power load. This implies that a great share of the part load ability of the turbomachinery – dependent on the operating CAS pressure difference – is consumed to provide a constant power consumption. Thus, the minimum electrical power consumption (62 % of nominal load) of the overall system is limited by the maximum applied storage pressure (100 bar in this case). Consequently, reducing the upper storage pressure leads to a better part load ability of the A-CAES system but also to a reduction of the exergy density.

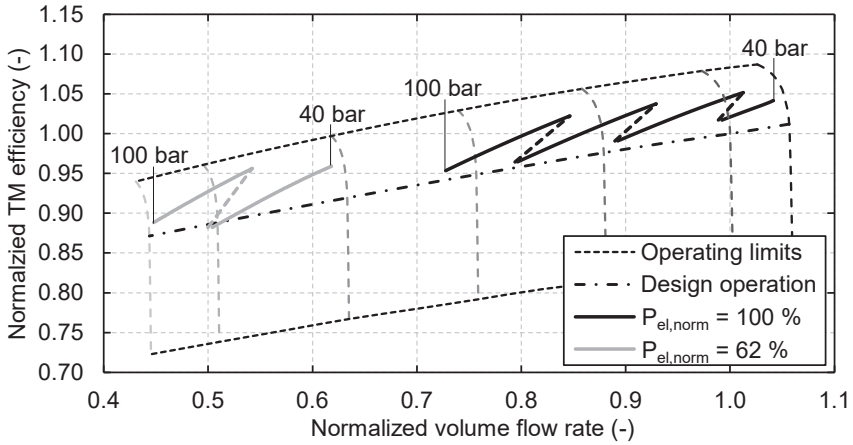

Figure 6. Efficiency map in the compression mode of the three-stage turbomachine and operating curve of the KompEx LTA-CAES® during charging process at minimum (62 % of nominal load) and maximum (100 % of nominal load) power consumption.

5. Conclusion

The introduced KompEx LTA-CAES® is able to efficiently realize wide CAS pressure ranges by the synergized use of turbo- and piston machines and appropriate control systems. Concretely, this is done by continuously varying the guide vanes of the turbomachines and a discrete control system to switch off single piston cylinders during the charging process. This offers an advantage compared to traditional A-CAES concepts using only turbomachines, especially when considering decentralized storage applications where artificial CAS technologies instead of salt caverns are usually suitable. For these applications, a high exergy density can have a decisive influence on the investment costs of the CAS volume and thus on the profitability of the overall system.

The strong fluctuations of process parameters during charging process (Figure 5) could be reduced by using piston cylinders with smaller swept volumes. Besides to the mass flow variation, the fluctuating intermediate pressure in particular is resulting to an operation of both machine types apart their design values. In order to realize a constant intermediate pressure and avoid discrete process fluctuations, a continuous control unit in the piston machinery train could be used, e. g. by implementing a variable speed control. This would lead to a more precise control and thus more efficient operation of the turbo and piston machines.

The operation behaviour of the reversibly operable turbo- and piston machines considered in this paper are derived from detailed CFD simulations within the KompEx project. In order to validate the respective data points, a test facility of the reversibly operable turbomachine is currently under construction.

Acknowledgments

The authors thank the German Federal Ministry for Economic Affairs and Climate Action for funding the project »KompEx LTA-CAES® modular« (FKZ 03ET6070A).

https://doi.org/10.52202/069564-0190

Appendix A

Table A.1. Overview of thermodynamically investigated A-CAES plant layouts sorted by increasing storage temperature.

Nr.	Literature[1]	$P_{el,in}$ MW_{el}	$P_{el,out}$ MW_{el}	$p_{CAS,min-max}$ bar	t_{TES} °C	η_{CAES} %AC-AC	TES-Medium	CAS[2]
1	[26]	N/A	0,7	8	60	52.90	Water	UW
2	[27]	8.1	8,6	75–125	90	52.00	Water	Artificial
3	[13]	N/A	0,5	17–80	92	41.00	Water	N/A
4	[28][1]	52.1	28.8	150	95	51.98	Water	Cavern
5	[29][1]	1.6	1.4	10–20	95	59.90	Water	N/A
6	[30][1]	0.4	2,0	46–66	100	58.90	Water	Cavern
7	[11][1]	27.1	19.2	42–70	100	66.17	Water	N/A
8	[31]	16.6	17.7	21–55	110	55.00	Water	Cavern
9	[32][1]	1.0	1.0	20–140	116	60.36	Water	Artificial
10	[33][1]	1.1	0.9	40–130	120	62.69	Oil	N/A
11	[28][1]	52.1	28.8	150	140	56.31	Water	Cavern
12	[7]	51.0	29	125–145	150	56.40	Water	Cavern
13	[34][1]	N/A	0.5	3–100	150	51.55	Water	Cavern
14	[23]	2.0	1.0	40–100	166	55.53	Water/ Concrete	Artificial
15	[12][1]	6.0	9.6	70–100	167	66.08	Water	N/A
16	[35][1]	17.7	5.3	25–64	176	60.27	N/A	N/A
17	[36][1]	83.3	96.0	40-60	178	57.14	Oil	N/A
18	[28][1]	52.1	28.8	150	180	59.07	Water	Cavern
19	[37][1]	26.0	14.4	120–155	189	54.25	Oil	Artificial
20	[38]	270.0	140.0	20–81	190	53.30	Water	Cavern
21	[15]	N/A	N/A	87–142	195	49.77	Oil	Cavern
22	[39]	85.5	131.5	140	216	56.70	Water	N/A
23	[40]	5.0	4.6	25–125	217	62.67	N/A	N/A
24	[41][1]	8.3	7.7	40–75	289	59.90	Rock	LRC
25	[19]	1.1	0.9	45–200	298	42.33	Oil	Artificial
26	[42]	60.0	110.0	70–100	300	55.40	Oil	Cavern
27	[43]	103.0	140.0	50–70	300	64.70	N/A	Cavern
28	[16]	60.0	161.0	43–70	300	50.00	Oil	Cavern
29	[44][1]	76.0	49.9	140	310	64.51	Water/PCM	Cavern
30	[45][1]	2.1	1.9	42–72	313	65.87	Oil	N/A
31	[46]	N/A	60.0	65–80	320	60.00	N/A	Cavern
32	[17]	N/A	N/A	20–70	327	52.25	Rock	N/A
33	[47]	60.0	40,7	72	337	63.31	N/A	LRC
34	[48]	70.0	40.0	40–65	380	68.00	Molten salt	Cavern
35	[49][1]	164.2	109.9	82.7	400	63.31	Oil	Cavern
36	[18]	0.1	0.0	4–20	410	52.07	Rock	N/A
37	[50][1]	0.5	N/A	20–80	440	65.43	Rock	Artificial
38	[51][1]	N/A	110.4	166	450	63.13	Oil	N/A
39	[49][1]	164.2	109.9	83	538	64.70	Oil	Cavern
40	[4]	N/A	N/A	28	550	68.50	Rock	LRC
41	[48]	70.0	40.0	40–65	580	68.70	Molten salt	Cavern
42	[52][1]	52.1	96.0	60–100	600	68.20	Rock	Cavern
43	[53][1]	N/A	N/A	10–100	600	64.51	N/A	N/A
44	[54][1]	104.2	96.0	46–66	600	64.70	Rock	Cavern

[1] The calculation of the cycle efficiency in thermodynamic studies is often not uniform. Many studies are only calculating the thermal efficiency resp. are neglecting mechanical and electrical losses. For a better comparability, the thermal efficiency in the marked sources is converted to the electrical cycle efficiency by assuming an electrical conversion efficiency of 0.96 for the charging and discharging process. In the respective sources, the charging and discharging power are also converted to electrical powers using the same factor.
[2] UW = underwater balloon, also called energy bag; Artificial: e. g. steel pipes or steel vessels; LRC = Lined Rock Cavern

Nr.	Literature[1]	$P_{el,in}$ MW_{el}	$P_{el,out}$ MW_{el}	$p_{CAS,min-max}$ bar	t_{TES} °C	η_{CAES} %AC-AC	TES-Medium	CAS[2]
45	[55][1]	104.2	211.2	46–72	632	68.20	Rock	Cavern
46	[56]	N/A	300.0	≤100	640	70.00	Rock	Cavern
47	[49][1]	164.2	109.9	82.7	649	67.09	Oil	Cavern
48	[57]	300.0	300.0	100–150	668	61.00	N/A	Cavern
49	[58]	N/A	100.0	120	N/A	56.60	Water	Artificial
50	[59]	80.0	100.0	40–80	N/A	54.50	Oil	N/A
51	[60]	0.8	0.6	42–85	N/A	55.50	Oil	N/A

References

[1] Hydrostor, Ed., "Hydrostor Activates World's First Utility-Scale Underwater Compressed Air Energy Storage System," Press Release, 2015.

[2] S. Mei et al., "Design and engineering implementation of non-supplementary fired compressed air energy storage system: TICC-500," Sci. China Technol. Sci., vol. 58, no. 4, pp. 600–611, 2015, doi: 10.1007/s11431-015-5789-0.

[3] J. Wang et al., "Overview of Compressed Air Energy Storage and Technology Development," Energies, vol. 10, no. 7, p. 991, 2017, doi: 10.3390/en10070991.

[4] L. Geissbühler et al., "Pilot-scale demonstration of advanced adiabatic compressed air energy storage, Part 1: Plant description and tests with sensible thermal-energy storage," Journal of Energy Storage, vol. 17, pp. 129–139, 2018, doi: 10.1016/j.est.2018.02.004.

[5] Hydrostor, "Projects," 2021. Accessed: Aug. 24 2021. [Online]. Available: https://www.hydrostor.ca/projects/

[6] Z. Tong, Z. Cheng, and S. Tong, "A review on the development of compressed air energy storage in China: Technical and economic challenges to commercialization," Renewable and Sustainable Energy Reviews, vol. 135, p. 110178, 2021, doi: 10.1016/j.rser.2020.110178.

[7] M. Budt, Thermodynamische Analyse adiabater Druckluftenergiespeicher unter Berücksichtigung feuchter Luft und Wassereinspritzung mittels dynamischer Simulation. Dissertation. Oberhausen: Karl Maria Laufen, 2016.

[8] M. Budt, D. Wolf, R. Span, and J. Yan, "A Review on Compressed Air Energy Storage: Basic principles, past milestones and recent developments," Applied Energy, vol. 170, pp. 250–268, 2016, doi: 10.1016/j.apenergy.2016.02.108.

[9] D. K. Kreid, "Technical and Economic Feasibility Analysis of the No-Fuel Compressed Air Energy Storage Concept," Pacific Northwest Laboratories, Richland, WA BNWL-2065 UC-94b, 1976.

[10] D. Wolf and M. Budt, "LTA-CAES – A low-temperature approach to Adiabatic Compressed Air Energy Storage," Applied Energy, vol. 125, pp. 158–164, 2014, doi: 10.1016/j.apenergy.2014.03.013.

[11] C. Guo et al., "Comprehensive exergy analysis of the dynamic process of compressed air energy storage system with low-temperature thermal energy storage," Applied Thermal Engineering, vol. 147, pp. 684–693, 2019, doi: 10.1016/j.applthermaleng.2018.10.115.

[12] H. Guo, Y. Xu, C. Guo, Y. Zhang, H. Hou, and H. Chen, "Off-design performance of CAES systems with low-temperature thermal storage under optimized operation strategy," Journal of Energy Storage, vol. 24, p. 100787, 2019, doi: 10.1016/j.est.2019.100787.

[13] W. Zhang, X. XUE, F. Liu, and S. Mei, "Modelling and experimental validation of advanced adiabatic compressed air energy storage with off-design heat exchanger," IET Renewable Power Generation, vol. 14, no. 3, pp. 389–398, 2020, doi: 10.1049/iet-rpg.2019.0652.

[14] Y. He, H. Chen, Y. Xu, and J. Deng, "Compression performance optimization considering variable charge pressure in an adiabatic compressed air energy storage system," Energy, 2018, doi: 10.1016/j.energy.2018.09.168.

[15] M. Dooner and J. Wang, "Potential Exergy Storage Capacity of Salt Caverns in the Cheshire Basin Using Adiabatic Compressed Air Energy Storage," Entropy, vol. 21, no. 11, p. 1065, 2019, doi: 10.3390/e21111065.

[16] L. Szablowski, P. Krawczyk, K. Badyda, S. Karellas, E. Kakaras, and W. Bujalski, "Energy and exergy analysis of adiabatic compressed air energy storage system," Energy, vol. 138, pp. 12–18, 2017, doi: 10.1016/j.energy.2017.07.055.

[17] H. Peng, Y. Yang, R. Li, and X. Ling, "Thermodynamic analysis of an improved adiabatic compressed air energy storage system," Applied Energy, vol. 183, pp. 1361–1373, 2016, doi: 10.1016/j.apenergy.2016.09.102.

https://doi.org/10.52202/069564-0190

[18] W. He et al., “Study of cycle-to-cycle dynamic characteristics of adiabatic Compressed Air Energy Storage using packed bed Thermal Energy Storage,” Energy, vol. 141, pp. 2120–2134, 2017, doi: 10.1016/j.energy.2017.11.016.

[19] S. Mucci, A. Bischi, S. Briola, and A. Baccioli, “Small-scale adiabatic compressed air energy storage: Control strategy analysis via dynamic modelling,” Energy Conversion and Management, vol. 243, p. 114358, 2021, doi: 10.1016/j.enconman.2021.114358.

[20] M. Sterner and I. Stadler, Eds., Energiespeicher - Bedarf, Technologien, Integration, 2nd ed. Berlin: Springer Vieweg, 2017. [Online]. Available: http://dx.doi.org/10.1007/978-3-662-48893-5

[21] J. Witte, Ed., Zentrale und dezentrale Elemente im Energiesystem: Der richtige Mix für eine stabile und nachhaltige Versorgung : Stellungnahme, 2020th ed. München, Halle (Saale), Mainz: acatech - Deutsche Akademie der Technikwissenschaften e. V; Deutsche Akademie der Naturforscher Leopoldina e.V. - Nationale Akademie der Wissenschaften; Union der deutschen Akademien der Wissenschaften e. V, 2020.

[22] M. Budt, M. Hadam, N. Kienzle, and E. Schischke, “Schlussbericht zum Verbundvorhaben KompEx LTA-CAES® modular: Entwicklung eines modularen Niedertemperatur-Druckluftenergiespeichers mit umkehrbar betreibbaren Maschinensätzen,” 2021.

[23] M. Hadam, “Thermodynamische Analyse eines modularen A-CAES mit umkehrbar betreibbaren Turbo- und Kolbenmaschinen,” Dissertation, Ruhr-Universität Bochum, Fakultät für Maschinenbau, Bochum, 2021.

[24] FNN, “TransmissionCode 2007: Anforderungen für die Umsetzung des SRL-Poolkonzepts zwischen ÜNB und Anbietern,” Anahng D2, Teil 2, Berlin, Nov. 2009.

[25] D. ÜNB, “Präqualifikationsverfahren für Regelreserveanbieter,” 2020.

[26] M. Ebrahimi, R. Carriveau, D. S.-K. Ting, and A. McGillis, “Conventional and advanced exergy analysis of a grid connected underwater compressed air energy storage facility,” Applied Energy, vol. 242, pp. 1198–1208, 2019, doi: 10.1016/j.apenergy.2019.03.135.

[27] F. Buffa, S. Kemble, G. Manfrida, and A. Milazzo, “Exergy and Exergoeconomic Model of a Ground-Based CAES Plant for Peak-Load Energy Production,” Energies, vol. 6, no. 3, pp. 1050–1067, 2013, doi: 10.3390/en6021050.

[28] C. Doetsch, M. Budt, D. Wolf, and A. Kanngießer, “Adiabates Niedertemperatur-Druckluftspeicherkraftwerk zur Unterstützung der Netzintegration von Windenergie,” Final report, Oberhausen, 2012.

[29] K. Yang, Y. Zhang, X. Li, and J. Xu, “Theoretical evaluation on the impact of heat exchanger in Advanced Adiabatic Compressed Air Energy Storage system,” Energy Conversion and Management, vol. 86, pp. 1031–1044, 2014, doi: 10.1016/j.enconman.2014.06.062.

[30] X. Luo et al., “Feasibility study of a simulation software tool development for dynamic modelling and transient control of adiabatic compressed air energy storage with its electrical power system applications,” Applied Energy, vol. 228, pp. 1198–1219, 2018, doi: 10.1016/j.apenergy.2018.06.068.

[31] X. Luo et al., “Modelling study, efficiency analysis and optimisation of large-scale Adiabatic Compressed Air Energy Storage systems with low-temperature thermal storage,” Applied Energy, vol. 162, pp. 589–600, 2016, doi: 10.1016/j.apenergy.2015.10.091.

[32] G. Grazzini and A. Milazzo, “A Thermodynamic Analysis of Multistage Adiabatic CAES,” Proc. IEEE, vol. 100, no. 2, pp. 461–472, 2012, doi: 10.1109/JPROC.2011.2163049.

[33] Y. He, MengWang, H. Chen, Y. Xu, and J. Deng, “Thermodynamic research on compressed air energy storage system with turbines under sliding pressure operation,” Energy, vol. 222, p. 119978, 2021, doi: 10.1016/j.energy.2021.119978.

[34] Y. He, H. Chen, Y. Xu, and J. Deng, “Compression performance optimization considering variable charge pressure in an adiabatic compressed air energy storage system,” Energy, vol. 165, pp. 349–359, 2018, doi: 10.1016/j.energy.2018.09.168.

[35] Z. Guo, G. Deng, Y. Fan, and G. Chen, “Performance optimization of adiabatic compressed air energy storage with ejector technology,” Applied Thermal Engineering, vol. 94, pp. 193–197, 2016, doi: 10.1016/j.applthermaleng.2015.10.047.

[36] Z. Han, S. Guo, S. Wang, and W. Li, “Thermodynamic analyses and multi-objective optimization of operation mode of advanced adiabatic compressed air energy storage system,” Energy Conversion and Management, vol. 174, pp. 45–53, 2018, doi: 10.1016/j.enconman.2018.08.030.

[37] T. Thomasson, “Dynamic Model Development of Adiabatic Compressed Air Energy Storage,” Master's Thesis, School of Energy Systems, Lappeenranta University of Technology, Jyväskylä, 2016.

[38] F. Uttke, “Modellierung eines adiabaten Druckluftspeichers in Modelica,” Masterarbeit, Institut für Energietechnik, Technische Universität Hamburg-Harburg, Hamburg, 2017.

[39] Y. Mazloum, H. Sayah, and M. Nemer, “Comparative Study of Various Constant-Pressure Compressed Air Energy Storage Systems Based on Energy and Exergy Analysis,” J. Energy Resour. Technol, vol. 143, no. 5, 2021, doi: 10.1115/1.4048506.

[40] A. Arabkoohsar, H. R. Rahrabi, A. S. Alsagri, and A. A. Alrobaian, “Impact of Off-design operation on the effectiveness of a low-temperature compressed air energy storage system,” Energy, vol. 197, p. 117176, 2020, doi: 10.1016/j.energy.2020.117176.

[41] J. Fan et al., “Thermodynamic and applicability analysis of a hybrid CAES system using abandoned coal mine in China,” Energy, vol. 157, pp. 31–44, 2018, doi: 10.1016/j.energy.2018.05.107.

[42] Helsingen, “Adiabatic compressed air energy storage,” Master's Thesis, Norwegian University of Science and Technology, Trondheim, 2015.

[43] Y. Huang et al., “Techno-economic Modelling of Large Scale Compressed Air Energy Storage Systems,” Energy Procedia, vol. 105, pp. 4034–4039, 2017, doi: 10.1016/j.egypro.2017.03.851.

[44] B. Ghorbani, M. Mehrpooya, and A. Ardehali, “Energy and exergy analysis of wind farm integrated with compressed air energy storage using multi-stage phase change material,” Journal of Cleaner Production, vol. 259, p. 120906, 2020, doi: 10.1016/j.jclepro.2020.120906.

[45] J.-L. Liu and J.-H. Wang, “A comparative research of two adiabatic compressed air energy storage systems,” Energy Conversion and Management, vol. 108, pp. 566–578, 2016, doi: 10.1016/j.enconman.2015.11.049.

[46] J. Bai et al., “Modelling and control of advanced adiabatic compressed air energy storage under power tracking mode considering off-design generating conditions,” Energy, vol. 218, p. 119525, 2021, doi: 10.1016/j.energy.2020.119525.

[47] S. Zhou, J. Zhang, W. Song, and Z. Feng, “Comparison Analysis of Different Compressed Air Energy Storage Systems,” Energy Procedia, vol. 152, pp. 162–167, 2018, doi: 10.1016/j.egypro.2018.09.075.

[48] D. Wolf, Methods for design and application of adiabatic compressed air energy: Storage based on dynamic modeling. Dissertation. Oberhausen: Karl Maria Laufen, 2011.

[49] V. de Biasi, “Fundamental analyses to optimize adiabatic CAES plant efficiencies,” Gas Turbine World, vol. 39, no. 5, Sep. 2009.

[50] E. Barbour, D. Mignard, Y. Ding, and Y. Li, “Adiabatic Compressed Air Energy Storage with packed bed thermal energy storage,” Applied Energy, vol. 155, pp. 804–815, 2015, doi: 10.1016/j.apenergy.2015.06.019.

[51] N. M. Jubeh and Y. S. Najjar, “Green solution for power generation by adoption of adiabatic CAES system,” Applied Thermal Engineering, vol. 44, pp. 85–89, 2012, doi: 10.1016/j.applthermaleng.2012.04.005.

[52] V. Tola, V. Meloni, F. Spadaccini, and G. Cau, “Performance assessment of Adiabatic Compressed Air Energy Storage (A-CAES) power plants integrated with packed-bed thermocline storage systems,” Energy Conversion and Management, vol. 151, pp. 343–356, 2017, doi: 10.1016/j.enconman.2017.08.051.

[53] H. Mozayeni, X. Wang, and M. Negnevitsky, “Exergy analysis of a one-stage adiabatic compressed air energy storage system,” Energy Procedia, vol. 160, pp. 260–267, 2019, doi: 10.1016/j.egypro.2019.02.145.

[54] H. Xue, “A comparative analysis and optimisation of thermo-mechanical energy storage technologies,” Apollo - University of Cambridge Repository, 2019.

[55] A. Sciacovelli et al., “Dynamic simulation of Adiabatic Compressed Air Energy Storage (A-CAES) plant with integrated thermal storage – Link between components performance and plant performance,” Applied Energy, vol. 185, pp. 16–28, 2017, doi: 10.1016/j.apenergy.2016.10.058.

[56] M. Bieber, R. Marquardt, and P. Moser, “The ADELE Project: Development of an Adiabatic CAES Plant Towards Marketability,” in 5th International Renewable Energy Storage Conference, Berlin, 2010.

[57] N. Hartmann, L. Eltrop, Bauer, N. Salzer, J, S. Schwarz, and M. Schmidt, “Stromspeicherpotentiale für Deutschland,” Universität Stuttgart, Stuttgart, Jul. 2012.

[58] Y. Mazloum, H. Sayah, and M. Nemer, “Exergy analysis and exergoeconomic optimization of a constant-pressure adiabatic compressed air energy storage system,” Journal of Energy Storage, vol. 14, pp. 192–202, 2017, doi: 10.1016/j.est.2017.10.006.

[59] Z. Han, Y. Sun, and P. Li, “Thermo-economic analysis and optimization of a combined cooling, heating and power system based on advanced adiabatic compressed air energy storage,” Energy Conversion and Management, vol. 212, p. 112811, 2020, doi: 10.1016/j.enconman.2020.112811.

[60] R. Jiang, Z. Cai, K. Peng, and M. Yang, “Thermo-economic analysis and multi-objective optimization of polygeneration system based on advanced adiabatic compressed air energy storage system,” Energy Conversion and Management, vol. 229, p. 113724, 2021, doi: 10.1016/j.enconman.2020.113724.

 https://doi.org/10.52202/069564-0190